IDEA League

Master of Science in Applied Geophysics

Research Thesis

Marchenko Inversion

Semih Demir

September 19, 2018

Marchenko Inversion

Master of Science Thesis

for the degree of Master of Science in Applied Geophysics at
Delft University of Technology
ETH Zürich
RWTH Aachen University
by

Semih Demir

September 19, 2018

Department of Geoscience & Engineering · Delft University of Technology
Department of Earth Sciences · ETH Zürich
Faculty of Georesources and Material Engineering · RWTH Aachen University

Delft University of Technology

Printed in The Netherlands

IDEA LEAGUE
JOINT MASTER'S IN APPLIED GEOPHYSICS

Delft University of Technology, The Netherlands
ETH Zürich, Switzerland
RWTH Aachen, Germany

Dated: *September 19, 2018*

Supervisor(s):

Prof. Dr. Evert Slob

Bingkun Yang

Committee Members:

Prof. Dr. Evert Slob

Prof Dr. Florian Wellmann

Bingkun Yang

Abstract

Marchenko inversion is a new way to invert seismic or electromagnetic data recorded during geophysical surveys. The inversion method uses Marchenko theory. This is a recent development which enables the retrieval of Green's functions at any place in the subsurface. A non-recursive Marchenko inversion method has already been introduced but in this thesis a recursive Marchenko inversion method is implemented and analysed. A recursive scheme lies at the center of this new method. In this thesis, the new method is implemented and tested on a 1D subsurface model. The recursive scheme is first validated. This is done by computing a reflection response with it and comparing it with a reflection response resulting from forward modeling. After this, the accuracy of retrieved local reflection coefficients from the recursive inversion method is determined. This is done by comparison with exact reflection coefficients of the subsurface model. After this, several different parameters of the used subsurface model, data computation and the recursive inversion method itself are investigated for their influence on the accuracy of the inversion method. In particular interest is the effect of interval time errors because these result in errors that can build up rapidly through the recursion. However, the method has a big advantage. It is shown that the recursive Marchenko inversion method has a way to retrieve the magnitude of made interval time errors and correct for these when interval times are overestimated. In this way the error build up is stopped. In the end, it is shown that the new method delivers high accuracy results and has an advantage in computational expense compared to the existing recursive Marchenko inversion method. It is concluded that the new method shows promising prospects and that it is worthwhile to investigate the method further.

Acknowledgements

An acknowledgement would not be one without thanking my supervisors, Evert Slob and Bingkun Yang. You have both been supportive of my work. Whenever I was stuck you have been helpful with guiding me in the right direction. I am very grateful for your help. Without your help, this thesis would have not been here. I would also like to say thank you to all the teachers that have taught me in the past years at TU Delft. Especially I would like to name Jan Dirk Jansen who supervised my Bachelor thesis and Guy Drijkoningen who made me realize I was interested in geophysics. I would like to thank my family and friends for their support and relieve from thesis work once in a while. I especially want to thank my father and mother for always being there for me for support and my sister Leyan, who helped me correct spelling mistakes at the end.

Delft University of Technology, The Netherlands — Semih Demir

September 19, 2018

Table of Contents

List of Figures

List of Tables

Acronyms

DUT Delft University of Technology

ETH Swiss Federal Institute of Technology

RWTH Aachen University

Chapter 1

Introduction

1-1 Background

Seismic imaging is a subject of exploration geophysics in which seismic data is being recorded at the surface of a medium with the goal to create an image of this medium. The main goal of creating this image is to gain an understanding of the structure of the earth and find resources such as hydrocarbons. Older methods of seismic imaging used only direct arrivals that are present in recorded data. These are arrivals that come from wave fields that traveled along the fastest path possible to the surface after being reflected at a certain point in the subsurface. A point of reflection lies at a boundary between geological layers in the subsurface, and it is this boundary that is also called a reflector. Multiple arrivals are wave arrivals that after reflecting due to a reflector didn't take the fastest route up to the surface where measurement takes place. Instead, these reflected wave fields have traveled a slower path due to reflection back into the subsurface taking place.

Studies have been done for a long time to be able to predict internal multiple arrivals. For example, in the paper [Hubral et al., 1980], the pattern of primary and multiple reflections that are observed after the addition of an extra reflector in the bottom of a series of reflectors was investigated.
More recently, ways to eliminate multiple arrivals such that only direct arrivals can be used have been found. One way of doing this, is by the use of a least-squares matching filter, in which a minimum-energy criterion is used to subtract predicted internal multiple data [Berkhout and Verschuur, 2005]. This has been shown to work on real data in numerous studies [Griffiths et al., 2011], [King et al., 2013], [Song et al., 2013], [Cypriano et al., 2015]. Another way to subtract predicted internal multiple arrivals is by using the third and higher order terms in the the inverse scattering series (ISS) [Weglein et al., 1997] and [Matson et al., 1999].

Multiple arrivals can also be used but then complications arise. In this case it is necessary to have receivers around the whole medium which illuminate it from all sides [Oristaglio, 1989] and [Fleury, 2012]. This is not the case in practice. To solve this, Green's functions can be used. A Green's function is the response of a medium to an illuminating point or point source at a specified location [Stakgold and Holst, 2011]. A novel way of retrieving these Green's functions, is by using Marchenko redatuming.

In short, Marchenko redatuming is a process in which wavefields are focused at a specified point in a medium. A 1D focused wavefield in an unknown medium has been retrieved by solving the Marchenko Equation [Rose, 2002]. The focusing point can act as a virtual source or as a virtual receiver. The focusing functions that are responsible for creating a focusing point are computed using the Marchenko redatuming equations from the reflection response.

The Green's function can be retrieved with the focusing functions and the reflection response. It has been shown that a Green's function can be retrieved by constructing a virtual receiver in a medium [Broggini et al., 2012]. A data driven wavefield focusing method to retrieve the Green's function was shown in [Broggini et al., 2014] and [Wapenaar et al., 2014]. The use of these Green's functions, measured at a virtual receiver in the subsurface, to create an image of the subsurface is called Marchenko Imaging. So, in Marchenko imaging, two wavefields are retrieved from the total reflection response. These are the focusing wavefield and the Green's function. Several studies into extending the formulation to include free-surface multiples were done like [Singh et al., 2015] and [Singh et al., 2017].

Marchenko inversion is the inversion of seismic or electromagnetic data after reflection coefficients of reflectors in a medium have been retrieved using Marchenko theory. These local reflection coefficients of the target zone are retrieved using the focusing functions. These reflection coefficient values are then used to invert for medium density and velocity of layers in a medium in the case of seismic data. Marchenko inversion has been proven to be possible by using a non-recursive scheme before in [Slob and Wapenaar, 2014] in which 1D electromagnetic data recorded using GPR was used.

The existing non-recursive method of Marchenko inversion consists of first determining the upgoing and downgoing focusing functions by solving the coupled Marchenko equations. For solving these coupled Marchenko equations an unconditionally convergent iterative method like LSQR can be used. In this existing method, both the upgoing and downgoing focusing functions are computed at a range of imaging times, going through the subsurface. One limitation of this method is the computational cost involved in generating focusing functions at all depth levels of the subsurface.

1-2 Objective

In this thesis, a new method of Marchenko inversion is investigated. This method makes use of a recursive scheme that can be used to determine the focusing functions. The new method of recursive Marchenko inversion will retrieve the local reflection coefficients of reflectors in a target zone. In short, the methodology behind the new method can be summarized as follows. First the coupled Marchenko equations are solved to retrieve the focusing functions above a target zone and then the recursive scheme is used for retrieving the local reflection coefficients of the reflectors in the target zone. It is expected that this recursive Marchenko inversion method will result in a decrease in computational cost in comparison with the existing, non-recursive Marchenko inversion method. This is because instead of generating focusing functions at each point in the subsurface with an equation to solve each time, this new method retrieves focusing functions at each deeper reflector in a direct computation procedure.

The objective of this thesis is to develop, implement, validate and assess the new recursive Marchenko inversion method.

1-3 Outline

The set up of this thesis, consisting of 4 components, is shown in Figure 1-1. The first component, consisting of the the subsurface model and data computation, provides the reflection response. The second component, consisting of both the existing and new Marchenko inversion method, provides local reflection coefficients and the computational time. The third component consists of comparisons between the new Marchenko inversion method and both the existing method (denoted with C) and the exact solution (denoted with B). Furthermore, the new Marchenko method is validated by comparing reflection responses computed with both data computation and the recursive scheme (denoted with A). The last component consists of the assumptions for this set up. These assumptions are related to the parameters of the subsurface model(denoted with a), the data computation(denoted with b) and the methods (denoted with c).

The thesis is structured as follows. First, the theory used is given in chapter 2. This theory consists of existing Marchenko theory and the recursive scheme. In Chapter 3, methods used for Marchenko inversion will be explained. In chapter 4, numerical results will be given. These numerical results will both validate the new method and assess the accuracy of the new method. This assessment will be based on comparisons of the new method with both the existing method and the exact solution. Finally, in Chapter 6, this thesis will be concluded.

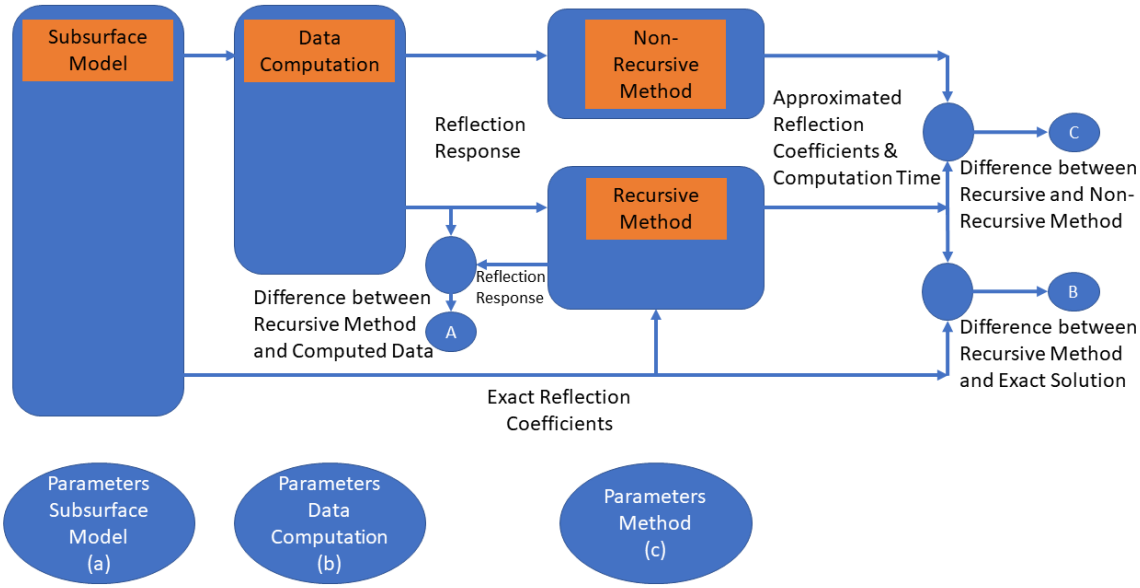

Figure 1-1: Set up of the thesis

Chapter 2

Theory

2-1 The Focusing Wavefield

Finding expressions for the focusing wavefield can be done by looking at a simple 3 layer medium with 2 reflectors as shown in Figure 2-1 from [Slob et al., 2014].

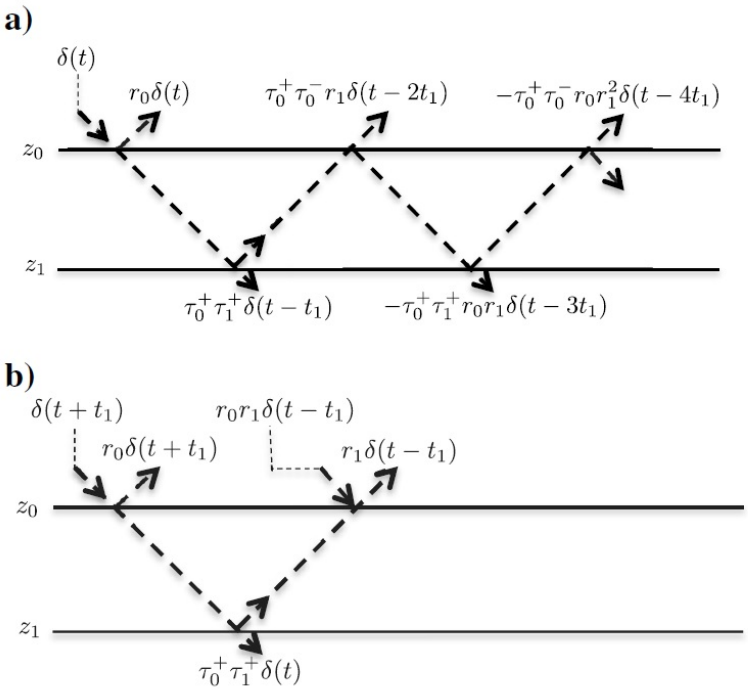

Figure 2-1: Reflection and transmission responses in a three layer model. In (a), no focusing takes place. In (b), focusing does take place. [Slob et al., 2014]

In Figure 2-1, the distance between z_0 and z_1 is given by $d_1 = z_1 - z_0$. The corresponding one-way travel time is given by $t_1 = d_1/c_1$. Local reflection and transmission coefficients are given by r_i, τ_i^+ and $-r_i, \tau_i^-$ in the case of downgoing and upgoing incident waves respectively. In Figure 2-1 (a), a normal incidence plane downgoing acoustic pressure wave, $\delta(t)$, is sent in just above z_0. The resulting upgoing field just above z_0 consists of an infinite number of events. The first two are primary reflections followed by a series of multiples [Slob et al., 2014]. The total upgoing field is called the impulse reflection response, $R(z_0, t)$ The downgoing wavefield below z_1 consists of a direct arrival followed by multiples. This is called the transmission response $T^+(z_1, z_0, t)$
In Figure 2-1 (b), it can be seen that a wavefield is created that does not have any multiple arrival anymore at z_0 and thus only one event at z_1. For this, a second downgoing wave has to be sent in to eliminate a second downgoing event below z_0 from occurring. The amplitude of this wave is $r_0 r_1$ and it reaches z_0 at $t = t_1$ [Slob et al., 2014]. Also, the incident wave is time advanced with the one-way travel time t_1. The result of these actions is that Figure 2-1 (b) creates a focused wavefield just below z_1 at time zero. The two downgoing waves together form the downgoing focusing wavefield. The general expression for the downgoing focusing wavefield is the inverse of the transmission response. The upgoing focusing wavefield is the resulting reflection response. This is shown below in Equation 2-1 and Equation 2-2. The individual waves that form the focusing wavefield can be distinguished on the most right hand side of Equation 2-1 and Equation 2-2.

$$f_1^+(z_0, z_1, \omega) = \frac{1}{T^+(z_1, z_0, \omega)} = \frac{e^{i\omega t_1} + r_0 r_1 e^{-i\omega t_1}}{\tau_0^+ \tau_1^+} \tag{2-1}$$

$$f_1^-(z_0, z_1, \omega) = \frac{R(z_0, \omega)}{T^+(z_1, z_0, \omega)} = \frac{r_0 e^{i\omega t_1} + r_1 e^{-i\omega t_1}}{\tau_0^+ \tau_1^+} \tag{2-2}$$

Important in Marchenko inversion is the knowledge that the latest event of the upgoing focusing wavefield has the amplitude of the reflection coefficient of the reflector just above the focusing point if the initial downgoing focusing function is an impulse. A unit amplitude focus can be constructed by sending in the inverse of the transmission response. In this case, the latest event of the upgoing focusing wavefield has the amplitude of reflection coefficient of the reflector just above the focusing point divided by the transmission coefficients of the reflectors above it. It is this amplitude focus that is called a focusing wavefield in the strict sense of Marchenko redatuming.

To focus a wavefield, a finite number of waves has to be sent in. The number of waves in the upgoing and downgoing focusing functions equals 2 to the power i, with i being the number of reflectors minus one [Slob et al., 2014]. Looking at the equations above, it can be seen that the division of the upgoing and downgoing focusing functions equals the measured reflection response as shown in Equation 2-3.

$$R(z_0, \omega) = \frac{f_1^-(z_0, z_1, \omega)}{f_1^+(z_0, z_1, \omega)} \tag{2-3}$$

Also important is the knowledge that the focusing functions for focusing at a certain depth level will be part of the focusing functions for a deeper depth level. Only the timing of the events is changed because focusing always takes place at zero time. This also means that

when the focusing depth level changes from just below a reflector to a lower level that is still above the next reflector, the amplitudes of the events in the focusing functions stay the same. Only the timing of the events is changed as a result of the focusing taking place at zero time. This can be illustrated as shown in Figure 2-2 below.

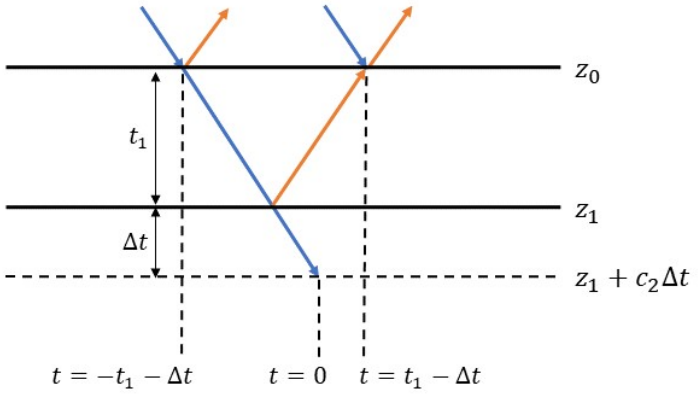

Figure 2-2: Focusing between 2 reflectors. Blue denotes downgoing ray paths. Orange denotes upgoing raypaths.

When focusing Δt c_{i+1} below a reflector z_i, the zero time changes to the new focusing depth. This results in a time shift of Δt of the events in the focusing functions in the time domain. In the frequency domain this means that the focusing functions can be represented as shown in Equation 2-4 and Equation 2-5.

$$f_1^+(z_0, z_{1+c_2\Delta t}, \omega) = \frac{1}{\tau_0^+ \tau_1^+} e^{i\omega(t_1+\Delta t)} + \frac{r_0 r_1}{\tau_0^+ \tau_1^+} e^{-i\omega(t_1-\Delta t)} \tag{2-4}$$

$$f_1^-(z_0, z_{1+c_2\Delta t}, \omega) = \frac{r_0}{\tau_0^+ \tau_1^+} e^{i\omega(t_1+\Delta t)} + \frac{r_1}{\tau_0^+ \tau_1^+} e^{-i\omega(t_1-\Delta t)} \tag{2-5}$$

The fact that focusing always takes place at zero time also means that when focus at a reflector z_i is achieved, the first event in the downgoing focusing function is timed at $t = -t_d(z_i, z_0)$ and the last event in the upgoing focusing functions is timed at $t = t_d(z_i, z_0)$. This means that the focusing functions are zero valued after $t = |t_d(z_i, z_0)|$

2-2 Green's Function Representation

Till now, the focusing functions were retrieved by solving the coupled Marchenko equations. Before the coupled Marchenko equations can be formed, first, two wavefield retrieval functions have to be defined. These are shown in the frequency domain in Equation 2-6 and Equation 2-7.

$$f_1^-(z_0, z_i, \omega) + G^{p,+}(z_0, z_i, \omega) = R(z_0, \omega) f_1^+(z_0, z_i, \omega) \tag{2-6}$$

$$[f_1^+(z_0, z_i, \omega)]^* - G^{p,-}(z_0, z_i, \omega) = R(z_0, \omega)[f_1^-(z_0, z_i, \omega)]^* \tag{2-7}$$

In Equation 2-6, the Green's function is retrieved that equals the impulse response caused by a downgoing wave at the focusing level z_i and is received at z_0. Equation 2-7 shows the retrieval of a Green's function that equals the impulse response caused by an upgoing wave at focusing level z_i and is received at z_0.

After transforming these equations to the time domain and rewriting them such that on the left hand side only the Green's function is present, they can be written as shown below in Equation 2-8 and Equation 2-9.

$$G^{p,+}(z_0, z_i, t) = -f_1^-(z_0, z_i, t) + \int_{t'=-t_d(z_i,z_0)}^{t} R(z_0, t - t^{'}) f_1^+(z_0, z_i, t^{'})\, \mathrm{d}t \tag{2-8}$$

$$G^{p,-}(z_0, z_i, t) = f_1^+(z_0, z_i, -t) - \int_{t'=-t_d(z_i,z_0)}^{t} R(z_0, t - t^{'}) f_1^-(z_0, z_i, -t^{'})\, \mathrm{d}t \tag{2-9}$$

The Green's function and reflection response are causal functions while the up and downgoing focusing functions are acausal. The Green's function is zero valued for $t < t_d(z_i, z_0)$. Since the focusing functions are zero valued for $|t| > t_d(z_i, z_0)$, the Green's function and focusing functions can be separated in time with the direct travel time to the focusing depth.

2-3 Coupled Marchenko Equations

The coupled Marchenko equations are now constructed as follows. First, the downgoing focusing function can be written as an addition of a first arrival of the transmission response and a multitude of arrivals after it which is called the coda. This is shown in Equation 2-10 and Equation 2-11.

$$\mathcal{T}_i = \prod_{j=0}^{i} \tau_j^+ \tag{2-10}$$

$$f_1^+(z_0, z_i, t) = \mathcal{T}_i^{-1}\delta(t + t_d(z_i, z_0)) + M^+(z_0, z_i, t) \tag{2-11}$$

Because $M^+(z_0, z_i, t) = 0$ and $f_1^-(z_0, z_i, t) = 0$ for $|t| \geq t_d(z_i, z_0)$ and $G^{\pm} = 0$ for $t < t_d(z - i, z_0)$ [Slob et al., 2014], Equation 2-8 and Equation 2-9 can be written as the coupled Marchenko equations shown in Equation 2-12 and Equation 2-13.

$$f_1^-(z_0, z_i, t) = \mathcal{T}_i^{-1}R(z_0, t + t_d(z_i, z_0)) + \int_{t'=-t_d(z_i,z_0)}^{t} M^+(z_0, z_i, t^{'})R(z_0, t - t^{'})\mathrm{d}t^{'} \tag{2-12}$$

$$M^+(z_0, z_i, -t) = \int_{t'=-t_d(z_i,z_0)}^{t} f_1^-(z_0, z_i, -t^{'})R(z_0, t - t^{'})\mathrm{d}t^{'} \tag{2-13}$$

The focusing functions can be determined by solving the coupled Marchenko equations iteratively. In this thesis the focusing functions are generated by using LSQR which is an unconditionally convergent iterative method.
This solver tries to solve a system of linear equations $Ax = b$ if A is consistent and otherwise attempts to solve the least squares solution x that minimizes $\|b - Ax\|^2$ In this system of linear equations, x contains the upgoing focusing wavefield and the coda of the downgoing focusing wavefield. A contains the reflection response. b contains the convolution of the first arrival of the downgoing focusing wavefield and the reflection response. Since A and b are known, x can be computed.

2-4 Recursive Relations for Focusing Functions

A recursive scheme can be used to construct focusing functions for a focusing point at a reflector. In a paper by [Robinson and Treitel, 1978], a similar recursive scheme was used to find reflection coefficients.
The recursive scheme for constructing focusing functions is shown below in Equation 2-14

$$\begin{bmatrix} f_1^+(z_0, z_i, \omega) \\ [f_1^-(z_0, z_i, \omega)]^* \end{bmatrix} = \frac{1}{\tau_i} \begin{bmatrix} e^{i\omega t_i} & r_i e^{-i\omega t_i} \\ r_i e^{i\omega t_i} & e^{-i\omega t_i} \end{bmatrix} \begin{bmatrix} f_1^+(z_0, z_{i-1}, \omega) \\ [f_1^-(z_0, z_{i-1}, \omega)]^* \end{bmatrix} \tag{2-14}$$

The recursive scheme can construct the focusing functions focused at a reflector given that the focusing functions of the previous reflector are known. Also, the reflection and transmission responses of the reflector have to be known together with the interval time of the reflector.
This means that this scheme is suitable for creating focusing functions for focusing points at a reflector while the non-recursive method of solving the coupled Marchenko equations can create focusing functions for a focusing point anywhere in the subsurface. It can be shown that the recursive scheme results in correct focusing functions by for example looking at a two layer model like in Figure 2-1. The starting focusing functions, $f_1^+(z_0, z_0, \omega)$ and $f_1^-(z_0, z_0, \omega)$, are given in Equation 2-15 and Equation 2-16.

$$f_1^+(z_0, z_0, \omega) = \frac{1}{\tau_0} \tag{2-15}$$

$$f_1^-(z_0, z_0, \omega) = \frac{r_0}{\tau_0} \tag{2-16}$$

This means that a unit amplitude focus will be achieved. The recursive scheme then results in an upgoing and a downgoing focusing function focusing at z_1 as shown in Equation 2-17 and Equation 2-18.

$$f_1^+(z_0, z_1, \omega) = \frac{1}{\tau_0^+ \tau_1^+} e^{i\omega t_1} + \frac{r_0 r_1}{\tau_0^+ \tau_1^+} e^{-i\omega t_1} \tag{2-17}$$

$$f_1^-(z_0, z_1, \omega) = \frac{r_0}{\tau_0^+ \tau_1^+} e^{i\omega t_1} + \frac{r_1}{\tau_0^+ \tau_1^+} e^{-i\omega t_1} \tag{2-18}$$

These equations are identical to Equation 2-1 and Equation 2-2. If now the model is extended with one more layer and the focusing functions for depth level z_2 were required to compute, the previous retrieved focusing functions for depth level z_1, Equation 2-17 and Equation 2-18, can be substituted in the recursive scheme.
This results in the focusing functions shown in Equation 2-19 and Equation 2-20.

$$\begin{aligned} f_1^+(z_0, z_2, \omega) &= \frac{1}{\tau_2} e^{i\omega t_2} \left[\frac{1}{\tau_0^+ \tau_1^+} e^{i\omega t_1} + \frac{r_0 r_1}{\tau_0^+ \tau_1^+} e^{-i\omega t_1} \right] + \frac{r_2}{\tau_2} e^{-i\omega t_2} \left[\frac{r_0}{\tau_0^+ \tau_1^+} e^{-i\omega t_1} + \frac{r_1}{\tau_0^+ \tau_1^+} e^{i\omega t_1} \right] \\ &= \frac{e^{i\omega(t_1+t_2)} + r_0 r_1 e^{i\omega(t_2-t_1)} + r_0 r_2 e^{i\omega(-t_1-t_2)} + r_1 r_2 e^{i\omega(t_1-t_2)}}{\tau_0^+ \tau_1^+ \tau_2^+} \\ &= \frac{1}{T^+(z_2, z_0, \omega)} \end{aligned} \tag{2-19}$$

$$f_1^-(z_0,z_2,\omega) = \frac{r_2}{\tau_2}e^{-i\omega t_2}\Big[\frac{1}{\tau_0^+\tau_1^+}e^{-i\omega t_1} + \frac{r_0 r_1}{\tau_0^+\tau_1^+}e^{i\omega t_1}\Big] + \frac{1}{\tau_2}e^{i\omega t_2}\Big[\frac{r_0}{\tau_0^+\tau_1^+}e^{i\omega t_1} + \frac{r_1}{\tau_0^+\tau_1^+}e^{-i\omega t_1}\Big]$$

$$= \frac{r_2 e^{i\omega(-t_1-t_2)} + r_0 r_1 r_2 e^{i\omega(t_1-t_2)} + r_0 e^{i\omega(t_1+t_2)} + r_1 e^{i\omega(t_2-t_1)}}{\tau_0^+\tau_1^+\tau_2^+}$$

$$= \frac{R(z_0,\omega)}{T^+(z_2,z_0,\omega)} \tag{2-20}$$

It is known that the reflection response recorded at the surface (z_0) and the transmission response for a source at z_0 and a receiver at z_2 generated by a unit amplitude plane wave are given by [Goupillaud, 1961]. These are shown in Equation 2-21 and Equation 2-22.

$$R^+(z_0,\omega) = \frac{r + r_1 e^{-2i\omega t_1} + r_2 e^{-2i\omega(t_1+t_2)} + r_0 r_1 r_2 e^{-2i\omega t_2}}{1 + r_0 r_1 e^{-2i\omega t_1} + r_0 r_2 e^{-2i\omega(t_1+t_2)} + r_1 r_2 e^{-2i\omega t_2}} \tag{2-21}$$

$$T^+(z_2,z_0,\omega) = \frac{\tau_0^+\tau_1^+\tau_2^+ e^{-i\omega(t_1+t_2)}}{1 + r_0 r_1 e^{-2i\omega t_1} + r_0 r_2 e^{-2i\omega(t_1+t_2)} + r_1 r_2 e^{-2i\omega t_2}} \tag{2-22}$$

The general expression for the downgoing focusing wavefield is the inverse of the transmission response and the upgoing focusing wavefield is the resulting reflection response. The focusing functions Equation 2-19 and Equation 2-20 resulting from the recursive scheme can be used to compute reflection and transmission responses (Equation 2-21 and Equation 2-22) that are given in [Goupillaud, 1961].

Chapter 3

Methods

3-1 Non-Recursive Method

The non-recursive method for Marchenko inversion can be schematically shown as in Figure 3-1.

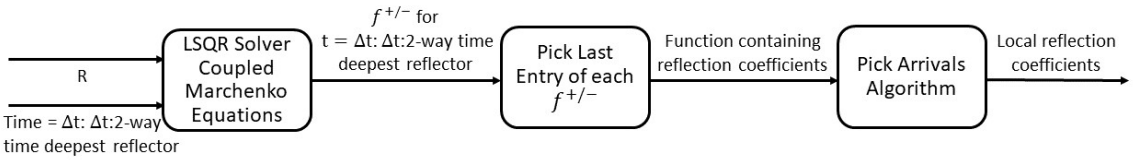

Figure 3-1: Schematic overview of the non-recursive Marchenko inversion method.

Looking at Figure 3-1, it can be seen that the non-recursive method used for Marchenko inversion consists of first solving the coupled Marchenko equations. In this research always the unconditionally convergent iterative LSQR method is used. Solving of the coupled Marchenko equations results in focusing functions for a specified time. A local reflection coefficient is retrieved by storing the final amplitude of the upward focusing function. Since it is not known where the layer boundaries/reflectors are, it is necessary to solve the coupled Marchenko equations at a number of times listed in an array. This means that in contrast with the new recursive Marchenko inversion method, the non-recursive Marchenko inversion method consists of solving the coupled Marchenko equations multiple times in a loop, storing the final amplitude of the upward focusing functions each time. Problems arise when the time step used for focusing is too big, causing a reflector to be skipped. This is illustrated in Figure 3-2. As can be seen in Figure 3-2, a too large time step between focusing times will result in a local reflection coefficient that cannot be retrieved by storing the final amplitude of the upgoing focusing function. This means that the local reflection coefficient of this

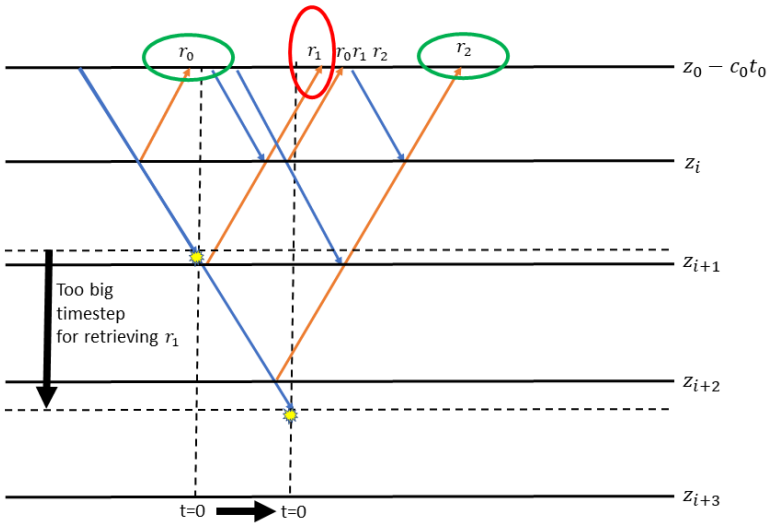

Figure 3-2: Illustration of a too large time step used to retrieve a local reflection coefficient, using the non-recursive Marchenko inversion method. The reflection coefficients retrieved and not retrieved are shown in green and red respectively. Only the amplitudes of the upgoing focusing functions are depicted.

reflector will not be retrieved. To mitigate this, a small enough time step for focusing has to be chosen. In this thesis, the non-recursive Marchenko inversion method used an array of focusing times from Δt till the two-way time of the deepest reflector in time steps of Δt. It is expected that this results in a higher computational cost for this method in contrast with the recursive Marchenko inversion method which automatically jumps from reflector to reflector in non-fixed time steps.

3-2 Recursive Method

In this thesis, a new recursive Marchenko inversion method is developed and implemented in which the coupled Marchenko equations are solved first by the unconditionally convergent iterative LSQR method. This results in created focusing functions for a focusing point above a zone of interest. Then, by substituting the new recursive scheme in the wavefield retrieval equation, given again in Equation 3-1, and rewriting it, the local reflection coefficients of the reflectors below are determined in a down going progression.
In Equation 3-1, the wavefield retrieval equation is shown again.

$$R(z_0,\omega)f_1^+(z_0,z_{i+1},\omega) = f_1^-(z_0,z_{i+1},\omega) + G^{p,+}(z_0,z_{i+1},\omega) \tag{3-1}$$

Now the focusing functions expressions from the recursive scheme are substituted in Equation 3-1. The result is shown in Equation 3-2.

$$\begin{aligned} R(z_0,\omega)\Big[f_1^+(z_0,z_i,\omega)e^{i\omega t_{i+1}} + r_{i+1}/\tau_{i+1})e^{-i\omega t_{i+1}}[f_1^-(z_0,z_i,\omega)]^*\Big] = \\ f_1^-(z_0,z_i,\omega)e^{i\omega t_{i+1}} + (r_{i+1})e^{-i\omega t_{i+1}}[f_1^+(z_0,z_i,\omega)]^* + \tau_{i+1}G^{p,+}(z_0,z_i,\omega) \end{aligned} \tag{3-2}$$

By rearranging the above equation to find an expression for the local reflection coefficient of reflector $i+1$, Equation 3-3 is found.

$$r_{i+1} = \frac{f_1^-(z_0,z_i,\omega)e^{i\omega t_{i+1}} - R(z_0,\omega)f_1^+(z_0,z_i,\omega)e^{i\omega t_{i+1}} + \tau_{i+1}G^{p,+}(z_0,z_i,\omega)}{R(z_0,\omega)e^{-i\omega t_{i+1}}[f_1^-(z_0,z_i,\omega)]^* - e^{-i\omega t_{i+1}}[f_1^+(z_0,z_i,\omega)]^*} \tag{3-3}$$

Notice in Equation 3-3 that the numerator and denominator are Green's functions that have been shifted in time. This is shown in Equation 3-4.

$$r_{i+1} = -\frac{G^{p,+}(z_0,z_i,\omega)}{G^{p,-}(z_0,z_i,\omega)}e^{2i\omega t_{i+1}} + \tau_{i+1}\frac{G^{p,+}(z_0,z_{i+1},\omega)}{G^{p,-}(z_0,z_i,\omega)}e^{2i\omega t_{i+1}} \tag{3-4}$$

From Equation 3-4 it can be seen that calculation of r_{i+1} equals 2 terms that are both a division of Green's functions.The Green's function $G^{p,+}(z_0,z_{i+1},\omega)$ is not known at the time of computation of r_{i+1} so this term we would like to be able to take out of the equation. Equation 3-4 can also be written in a form $\alpha(\omega)\ r_{i+1} = \beta(\omega)$ by multiplication with $G^{p,-}(z_0,z_i,\omega)$, as shown in Equation 3-5.

$$G^{p,-}(z_0,z_i,\omega)\ r_{i+1} = -G^{p,+}(z_0,z_i,\omega)e^{2i\omega t_{i+1}} + \tau_{i+1}G^{p,+}(z_0,z_{i+1},\omega)e^{2i\omega t_{i+1}} \tag{3-5}$$

In the time domain the term $\tau_{i+1}G^{p,+}(z_0,z_i,\omega)e^{2i\omega t_{i+1}}$ will become zero for times lower than the direct travel time to the focus depth $i+1$ because the Green's function is zero valued for earlier times. Using this property, Equation 3-5 is transformed to the time domain and a time window of $-t_d < t < t_d$ is applied. This yields the expression shown below in Equation 3-6 with $\mathcal{T} = t + 2t_{i+1}$.

$$r_{i+1} = \frac{f_1^-(z_0,z_i,\mathcal{T}) - \int_{t'=-t_d(z_i,z_0)}^{\mathcal{T}} R(z_0,\mathcal{T}-t')f_1^+(z_0,z_i,t')\,\mathrm{d}t}{-f_1^+(z_0,z_i,-\mathcal{T}) + \int_{t'=-t_d(z_i,z_0)}^{\mathcal{T}} R(z_0,\mathcal{T}-t')f_1^-(z_0,z_i,-t')\,\mathrm{d}t} \tag{3-6}$$

In the implementation of the method, an approximation has been made. This approximation is that the reflection response (R) used in Equation 3-3 has been changed. The entries of R have been replaced with zeros after a time of $2t_d$ in the time domain before R was transformed into the frequency domain. This R is from now on denoted with R'. This means that (3-3) is now an approximation shown in (3-7). This is because there are errors made by using the same cutoff for all of R when transforming R' to the frequency domain.

$$\sim r_{i+1} = \frac{f_1^-(z_0,z_i,\omega)e^{i\omega t_{i+1}} - R'(z_0,\omega)f_1^+(z_0,z_i,\omega)e^{i\omega t_{i+1}}}{R'(z_0,\omega)e^{-i\omega t_{i+1}}[f_1^-(z_0,z_i,\omega)]^* - e^{-i\omega t_{i+1}}[f_1^+(z_0,z_i,\omega)]^*} \tag{3-7}$$

r_{i+1} will be called a reflection coefficient function from now. In contrast with Equation 3-3, the numerator and denominator of equation Equation 3-7 are now a subset of Green's functions because of the use of R'. They are denoted with $G^{p,+\prime}(z_0,z_i,\omega)$ and $G^{p,-\prime}(z_0,z_i,\omega)$ These subsets of Green's functions contain the first arrival of the real Green's functions. Equation 3-7 will be called the recursive scheme + wavefield retrieval equation from now on. The result is that the reflection coefficient function can now be shown as in Equation 3-8

$$\sim r_{i+1} = -\frac{G^{p,+\prime}(z_0,z_i,\omega)}{G^{p,-\prime}(z_0,z_i,\omega)}e^{2i\omega t_{i+1}} \tag{3-8}$$

The maximum amplitude of Equation 3-8 will, provided that a correct interval time is found, always lie at zero time because the right interval time will shift the first arrival of the division of the subset Green's functions to time zero. The reflection coefficient of the reflector at $i+1$ is this maximum amplitude.
The found interval time t_{i+1} is not only used for the time shift in Equation 3-8 but also for the creation of $R^{'}$. This is because entries in R are (in the time domain) replaced by zeros after the 2-way travel time to reflector $i+1$. This means that when an overestimation of interval time t_{i+1} takes place, the subset Green's functions still contain the correct maximum amplitude arrival. However, they are shifted too far in Equation 3-8 which causes the maximum amplitude to lie at a negative times instead of at zero time. The size of the time shift from zero time into negative time equals the exact amount of overestimation of t_{i+1}. In the case of an underestimation an interval time t_{i+1}, the consequences are more severe. In this case the subset Green's functions do not contain the first arrival from reflector $i+1$ because the reflection response used for computing the subset Green's functions ($R^{'}$) does not contain enough data to include the first arrival from reflector $i+1$.

The theory outlined above translates in a methodology explained now. The recursive Marchenko inversion method is schematically shown, in Figure 3-3.

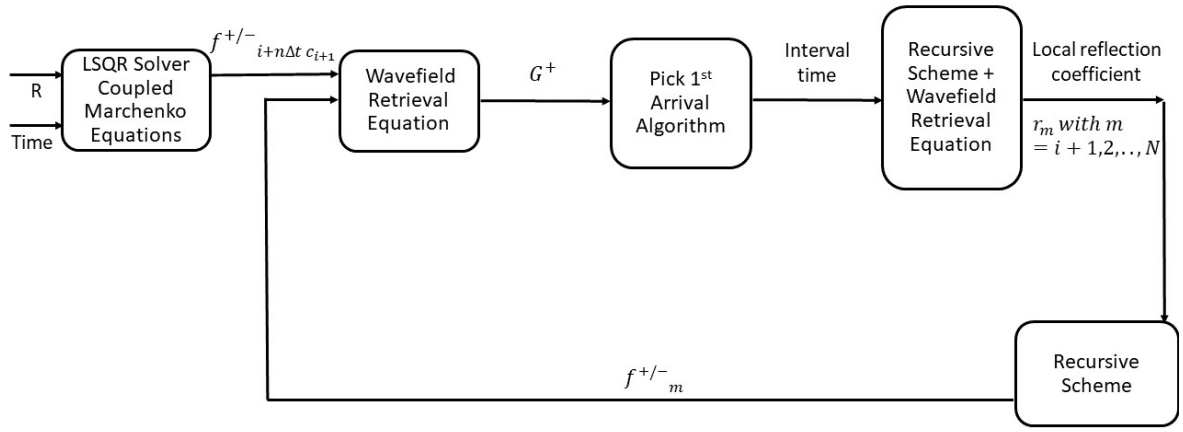

Figure 3-3: Schematic overview of the recursive Marchenko inversion method.

The first iteration of the method makes use of the LSQR method to solve the coupled Marchenko type equations and the recursive scheme + wavefield retrieval equation (Equation 3-7) to retrieve the first local reflection coefficient. The second till the final iteration will create new focusing functions at a reflector with the recursive scheme (Equation 2-14) and retrieve the local reflection coefficient of the next reflector by using Equation 3-7.

First the methodology in iterations 2 till N is explained. N is the total number of reflection coefficients retrieved with the method. In these iterations, no coupled Marchenko equations are solved. Only the recursive scheme (Equation 2-14), wavefield retrieval equation (Equation 3-1) and the recursive scheme + 1st wavefield retrieval equation (Equation 3-7) are used. After a local reflection coefficient r_{i+1} is retrieved, the recursive scheme (Equation 2-14) is used to compute focusing functions $f^{+/-}$ focused at z_{i+1}. The wavefield retrieval function (Equation 3-1) is used to compute the Green's function after which it is transformed to the

time domain resulting in $G^{p,+}(z_0 - c_0 t_0, z_{i+1}, t)$. The first arrival of the Green's function is picked with the pick 1st arrival algorithm. The interval time to the next reflector t_{i+2} is determined from the first arrival of the Green's function. Finally the recursive scheme + wavefield retrieval equation (Equation 3-7) is used to compute a new local reflection coefficient r_{i+1} and the next iteration is started.

The above explained iteration is visualized with ray paths shown in Figure 3-4. Also the next iteration is shown, in Figure 3-5.

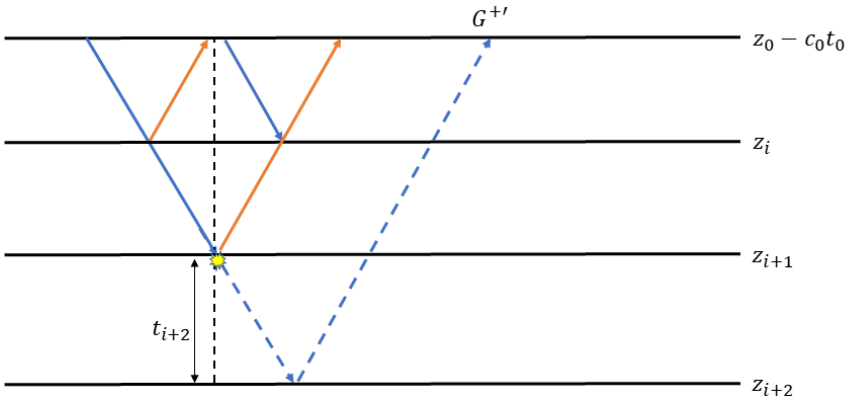

Figure 3-4: Second focusing point of the recursive Marchenko inversion Method. 'i' equals zero. Downgoing and upgoing focusing functions are depicted in blue and orange respectively. The first arrival of the Green's function is depicted in a blue dotted line.

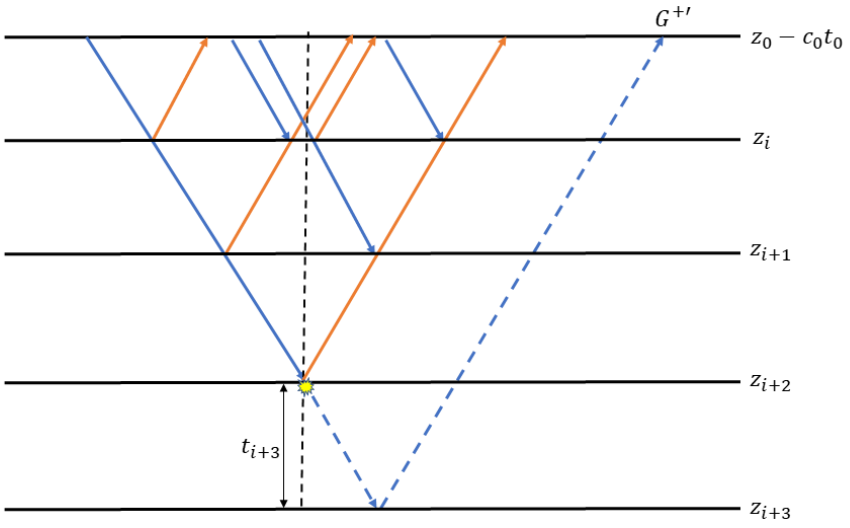

Figure 3-5: Third focusing point of the recursive Marchenko inversion method. 'i' equals zero. Downgoing and upgoing focusing functions are depicted in blue and orange respectively. The first arrival of the Green's function is depicted in a blue dotted line.

In these iterations, the focusing functions created with the recursive scheme do not need to

be shifted since each focusing point is situated at a reflector.

Now, the first iteration is explained. In this first iteration, there has been focused in between two reflectors. Since the recursive scheme can only create focusing functions at a reflector, this first iteration of the method is more complicated than iterations 2 till N as explained before. First, the coupled Marchenko equations are solved with LSQR to retrieve focusing functions for a focusing point at $i + n\Delta t\ c_{i+1}$. This is a depth just above a target zone. n is an integer that makes sure the point of focus is in between reflectors z_i and z_{i+1} The focusing functions are substituted in equation Equation 3-1 to compute the Green's function $(G^{+}(z_0 - c_0 t_0, z_i + n\Delta t\ c_{i+1}))$. From this Green's function, the one-way travel time from the focusing point at $z_i + n\Delta t\ c_{i+1}$ to the deeper lying reflector z_{i+1} is determined. This is done with Equation 3-9.

$$t_{i+1} - n\Delta t = \frac{t_{G^{+}(first)} - t_{focus}}{2} \tag{3-9}$$

In Equation 3-9 and Equation 3-10, t_{focus} denotes the focusing time, $t_{G^{+}(first)}$ denotes the time of the first arrival of the Green's function and $t_{f^{-}(last)}$ denotes the time of the last arrival in the upgoing focusing function. From the upgoing focusingfunction, the one-way traveltime from reflector z_i to the focusingpoint at $z_i + n\Delta t\ c_{i+1}$ is determined. This is being done with Equation 3-10.

$$n\Delta t = \frac{t_{focus} - t_{f^{-}(last)}}{2} \tag{3-10}$$

The interval time t_{i+1} in the first iteration of the recursive method is now found by adding the right hand sides of Equation 3-9 and Equation 3-10. Next, the up and downgoing focusing functions for the focusing point $z_i + n\Delta t\ c_{i+1}$ are shifted back in time to level z_i, using the earlier found time of $n\Delta t$. This results in focusing functions for a focusing point at reflector z_i. The recursive scheme + 1st wavefield retrieval equation (Equation 3-7), is now used to compute the reflection coefficient of reflector z_{i+1}.

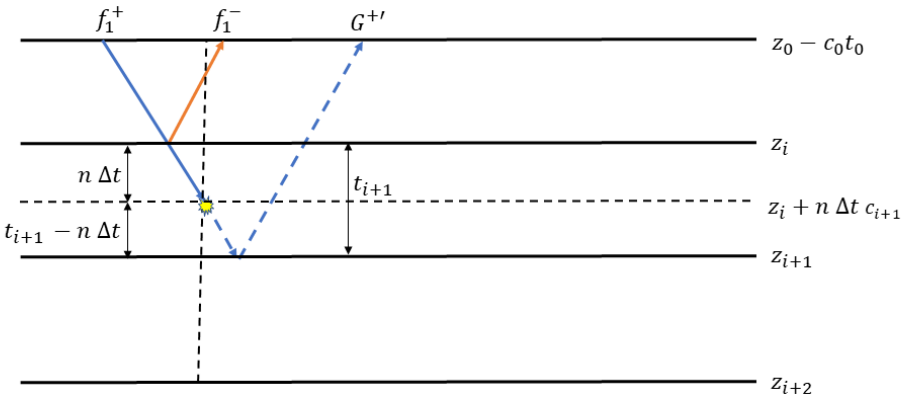

Figure 3-6: First focusing point of the recursive Marchenko inversion method. 'i' equals zero. Downgoing and upgoing focusing functions are depicted in blue and orange respectively. The first arrival of the Green's function is depicted in a blue dotted line.

The above explained first iteration is also shown in a visualization showing ray paths in Figure 3-6.

Chapter 4

Numerical Results

4-1 Processing Parameters

In this thesis, a 1D 11 layer model is used as a base subsurface model. The model properties are shown in Table 4-1. Effectively it acts as a 10 layer model in simulations because the 11th layer is of a height representing infinity for the simulations. The subsurface model can be changed by changing the heights, velocities and densities of the layers.

Layer	1	2	3	4	5	6	7	8	9	10	11
Velocity (m/s)	1500	1900	2100	1700	2100	2100	2100	2100	2500	2750	2900
Density (kg/m^3)	1.5	2.25	1.75	1.43	1.75	1.93	1.7	2.11	2.11	2.25	2.30
Height (m)	75	117	99	85	111	75	123	151	163	221	8e7

Table 4-1: Base subsurface model parameters

The reflection coefficients of the layer boundaries, shown in Table 4-2, are computed as part of a forward modeling step that only uses the subsurface model.

	1	2	3	4	5	6	7	8	9	10
r	-0.3103	0.0755	0.2037	-0.2037	-0.0489	0.0634	-0.1076	-0.0870	-0.0796	-0.0375

Table 4-2: Exact local reflection coefficients of the base subsurface model

The equation for computing local reflection coefficients is shown in Equation 4-1.

$$r = \frac{\rho_2 V_2 - \rho_1 V1}{\rho_2 V_2 + \rho_1 V1} \tag{4-1}$$

In Equation 4-1, ρ stands for the density in kg/m^3 and V stands for the velocity in m/s of a medium 1 and 2 with the reflector in between. This equation is only applicable in case of waves hitting a reflector with normal incidence because then the relationship shown in Equation 4-2 holds.

$$Z = \rho V \tag{4-2}$$

In Equation 4-2, Z stands for the acoustic impedance of a medium in $Pa\ s/m3$. The vertical incidence assumption is used throughout this thesis as is the fact that the subsurface model has piecewise constant acoustic impedances.
The total reflection response can be computed by forward modeling, taking into account the subsurface model and data computation parameters. In this step there are several parameters that can be changed. The geometry of the sources and receivers can be changed by setting them at different heights in the subsurface, creating a free surface above in return. In this case, the reflection coefficient of the free surface can be specified. The ghost effect can be taken into account when simulating marine seismic surveys. The wavelet generated by the sources can be changed with parameters such as the center frequency and the number of frequencies sampling point. These parameters in turn also influence variables like the time sampling interval Δt. In the recursive Marchenko inversion method, created functions are sometimes convolved with a Ricker wavelet. The base setting for these parameters assumed no free surface effects and thus also no ghosting, meaning that the sources and receivers were directly situated in the top of the first layer. A center frequency of 50Hz is chosen. The number of frequency sampling points is set as 16*8192. The base settings for data computation resulting in the total reflection response are shown in Table 4-3.

Parameter	Value
Height of sources (m)	0
Height of receivers (m)	0
Reflection coefficient, Free Surface (-)	0
Wavelet center frequency (Hz)	50
Number of frequency sampling point (-)	16*8192

Table 4-3: Base data computation parameters

The result of these parameters is that the time step used for numerical modelling, Δt, is of size 8.3333e-04 seconds.

The base recursive method parameters are selected to ensure that correct first arrivals in the Green's functions are picked. To ensure this, the pick first arrival algorithm, as shown in Figure 3-3 is constructed with 6 conditions that have to be met for an amplitude in the Green's function to be picked as first arrival. Because the Green's function has been convolved with a Ricker wavelet, each amplitude arrival consists of a main lobe with side lobes. The characteristics of these lobes is dependent on the Ricker wavelet chosen. The first condition is that the side lobes must be less than 50 time samples away from each other. The second is that the distances from the main lobe to the side lobes should not differ more than 30 percent. The third condition is that the side lobes should have the same sign. The 4th condition is that the side lobes have an opposite sign compared to the main lobe. The fifth condition is that the side lobes should not differ more than 30 percent in amplitude. The sixth and final condition is that the earliest main lobe with side lobes fulfilling the previous 5 conditions is chosen as first arrival of the Green's function. The parameters of the recursive Marchenko inversion method can be summarized as shown in Table 4-4.

Parameter	Value
Distance between side lobes (time samples)	50
Difference between side lobe to main lobe distances (percent)	30
Amplitude difference between side lobes (percent)	30

Table 4-4: Base recursive method parameters

4-2 Validation of Recursive Scheme

In this section, the recursive scheme is used for generating focusing functions and the reflection response as a result. This reflection response is then compared with the reflection response from data computation.
The goal behind this is to numerically validate the recursive scheme, introduced in equation Equation 2-14. As shown in the theory section, Equation 2-3, the total reflection response equals the division of the downgoing and upgoing focusing functions. Computing this total reflection response numerically by using the recursive scheme should yield the same function as forward modeling of the reflection response. The base subsurface model and base data computation parameters as shown before in table Table 4-1 and table Table 4-3, were used. This means that no free surface was used, resulting in receivers and sources that are placed on the first layer boundary. The starting focusing functions put into the recursive scheme were specified as shown in Equation 4-3 and Equation 4-4.

$$f_1^+(z_0 - c_0 t_0, z_0) = \frac{1}{\tau_0} e^{i\omega t_0} \tag{4-3}$$

$$[f_1^-(z_0 - c_0 t_0, z_0)]^* = [\frac{r_0}{\tau_0} e^{-i\omega t_0}]^* \tag{4-4}$$

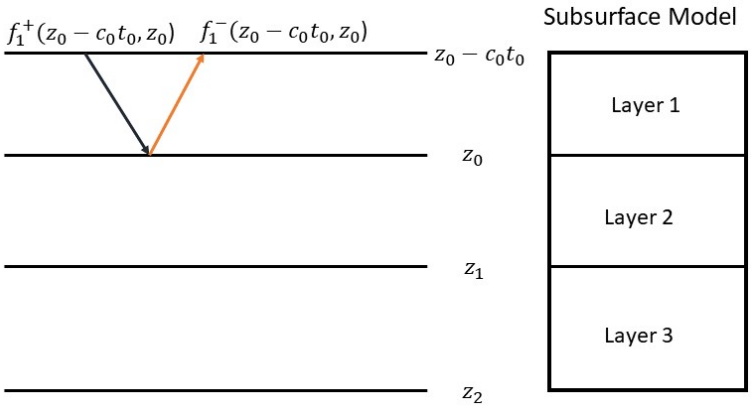

Figure 4-1: Starting focusing functions for recursion with as goal to validate the recursive scheme.

From Equation 4-3 and Equation 4-4, it can be seen that the receivers and sources are located on top of the first layer which is at a height of reflector $z_0 - c_0 t_0$. z_0 is the height of the first reflector and t_0 is the one-way travel time through the first layer. This is shown in Figure 4-1. In Figure 4-2, both the total reflection response created by forward modeling and the total reflection response created with the new recursive scheme are shown. In Figure 4-2, it can be seen that indeed, the two created total reflection responses are the same. After this validation and demonstration it was concluded that the recursive scheme is suitable for creating focusing functions and thus for implementation in the recursive Marchenko inversion method.

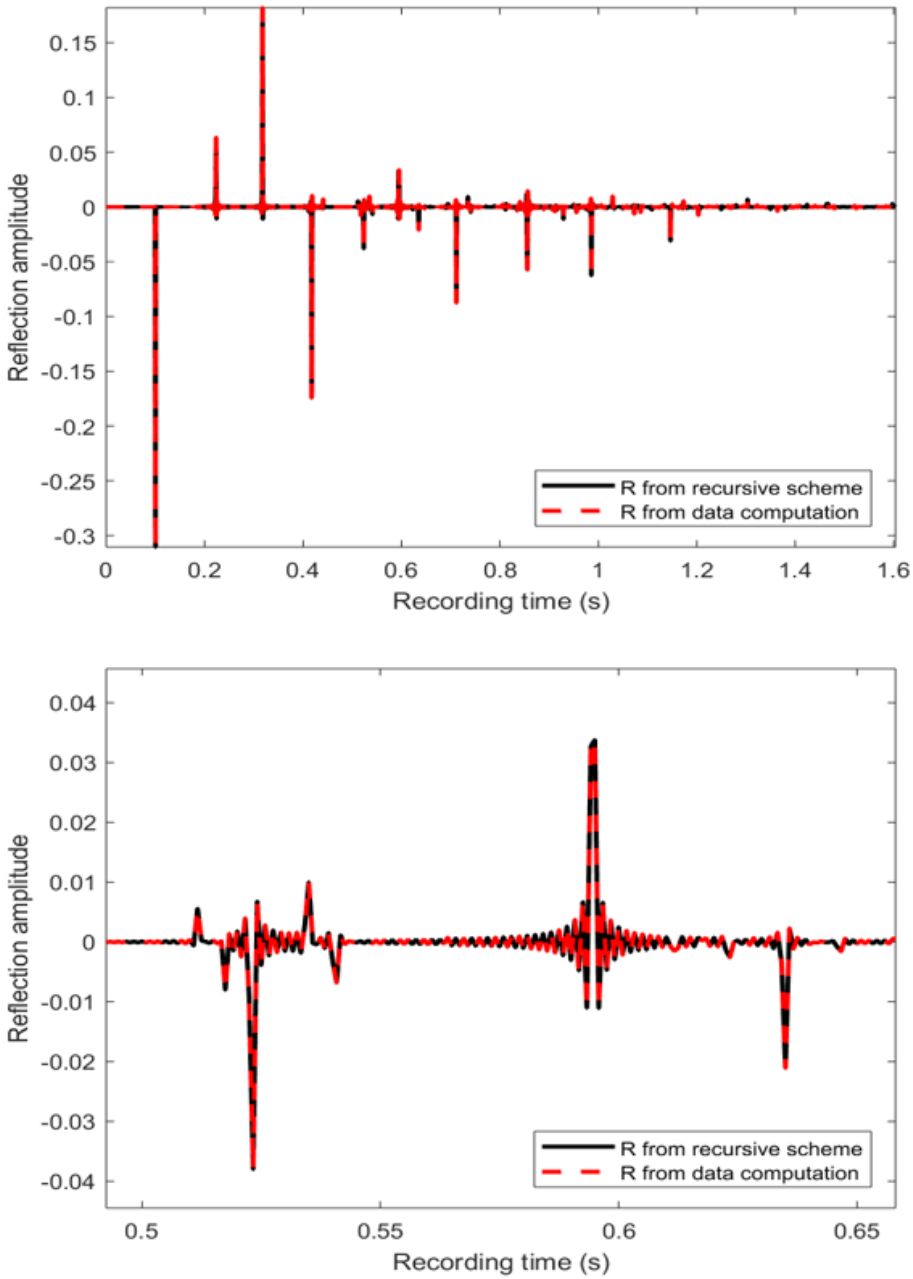

Figure 4-2: Total reflection response created by recursive scheme and data computation, shown in red and dotted black lines respectively. Lower half is a zoomed in version of the upper half.

4-3 Demonstration of Recursive Method

The new recursive Marchenko inversion method is demonstrated in two areas. These are retrieved Green's functions and reflection coefficient functions, with as objective to show that the recursive method is working sufficiently.

A figure showing a gather of all retrieved Green's functions is shown in Figure 4-3.

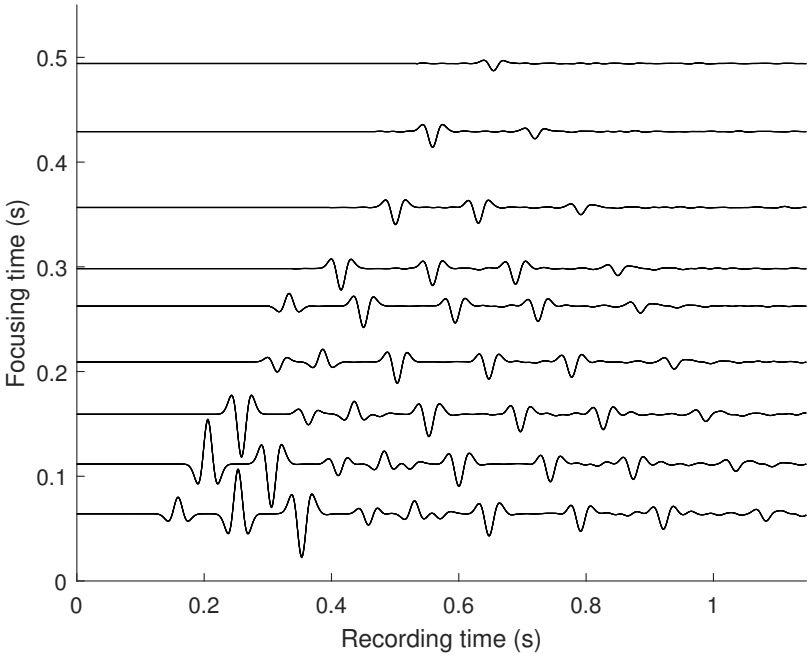

Figure 4-3: Gather of all retrieved Green's functions by the recursive Marchenko inversion method.

As can be seen in Figure 4-3, a clear relationship is visible in which each time there has been focused at a deeper lying reflector, the retrieved Green's function has it's first arrival at a later time which is to be expected since the travel time from the virtual source in the subsurface to the surface level becomes longer. Also note that the final retrieved Green's function seems to contain only one arrival, the primary arrival, with no multiple arrivals after it. In reality there are later arrivals but these have such small amplitudes that they are not visible in the above figure.

Now, the reflection coefficient function plots that contain the retrieved reflection coefficients are demonstrated. In Figure 4-4, the second retrieved reflection coefficient function is shown. This is the reflection coefficient function containing the reflection coefficient of reflector z_2. As can be seen in Figure 4-4, the maximum absolute amplitude of the function lies at time zero. This means that for this recursion, the correct interval time t_2 was retrieved. From the reflection coefficient function in Figure 4-4, the local reflection coefficient of 0.2 was retrieved for reflector z_2.

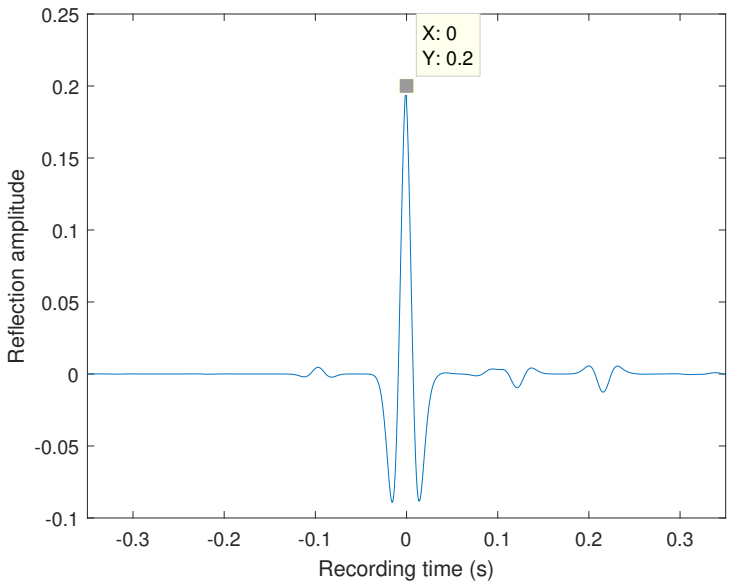

Figure 4-4: Second retrieved reflection coefficient function, containing the local reflection coefficient of reflector z_2.

Now, the influence of an interval time error on the created reflection coefficient function is demonstrated. For this, the interval time t_2 is being contaminated with either an over or an underestimation of $4\Delta t$. In Figure 4-5, the reflection coefficient function of reflector z_2 is plotted when the interval time t_2 is contaminated with an overestimation of $4\Delta t$. As can be seen in the reflection coefficient function shown in Figure 4-5, the maximum amplitude has been shifted away from time zero to a time of -0.00333 seconds. This is exactly $4\Delta t$.

In Figure 4-6, the reflection coefficient function of reflector z_2 is plotted when the interval time t_2 is contaminated with an underestimation of $4\Delta t$. As can be seen in the reflection coefficient function shown in Figure 4-6, there is no arrival present anymore that has the value of the local reflection coefficient of z_2 as amplitude.

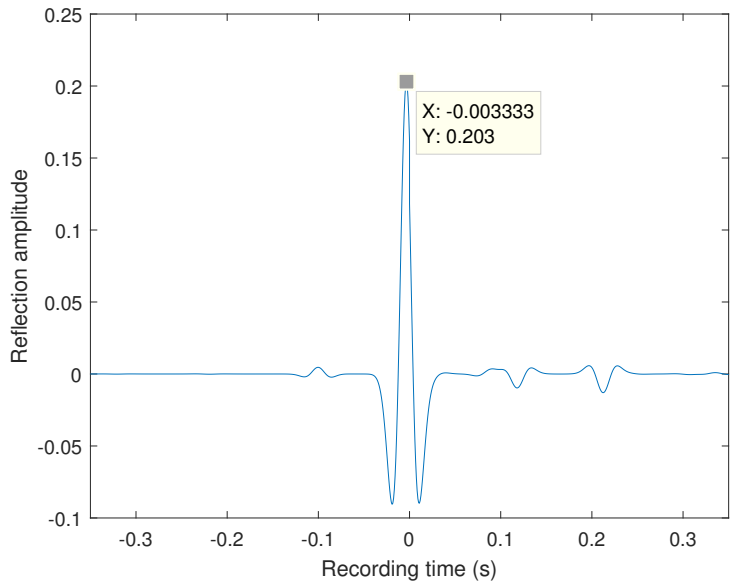

Figure 4-5: Second retrieved reflection coefficient function, containing the local reflection coefficient of reflector z_2. Interval time t_2 has been overestimated with $4\Delta t$.

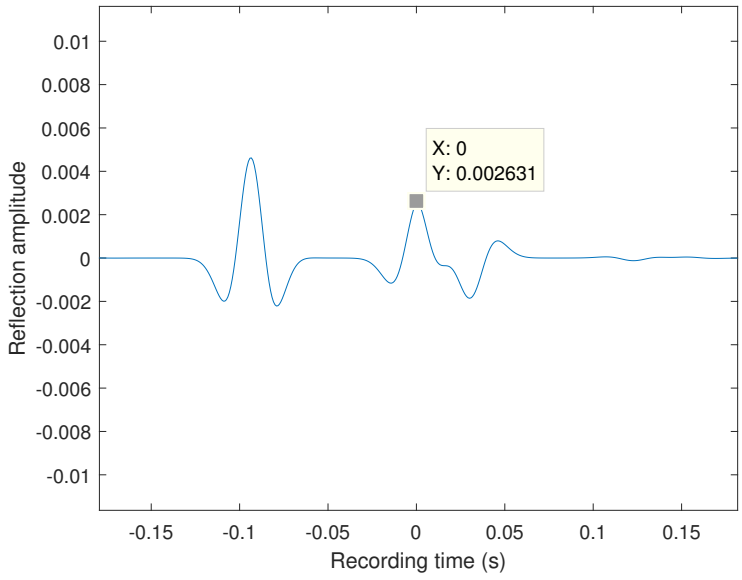

Figure 4-6: Second retrieved reflection coefficient function, containing the local reflection coefficient of reflector z_2. Interval time t_2 has been underestimated with $4\Delta t$.

4-4 Comparison between Recursive Method and Exact Solution

4-4-1 Base Model, Base Data Computation and Base Method Parameters

The local reflection coefficients retrieved with the recursive Marchenko inversion method are compared with the exact local reflection coefficients from the subsurface model. This is done under base subsurface model, data computation and recursive method parameters as specified in Table 4-1, Table 4-3 and Table 4-4.
In Table 4-5, the picked first arrival times of the Green's function retrieved by the pick first arrival algorithm are shown.

	1	2	3	4	5	6	7	8	9
time(s)	0.1592	0.2058	0.2583	0.3150	0.3333	0.4150	0.5008	0.5592	0.6542

Table 4-5: Picked first arrivals of the Green's functions. Base subsurface model, data computation and recursive method parameters are used.

The found times in Table 4-5, correspond with each first arrival in the Green's function gather in Figure 4-3.

These first arrival times are then used to retrieve the interval times. They are shown in Table 4-6, together with the exact interval times from forward modeling and percentage errors.

	t_1	t_2	t_3	t_4	t_5	t_6	t_7	t_8	t_9
time exact (s)	0.0616	0.0471	0.0500	0.0529	0.0357	0.0586	0.0719	0.0652	0.0804
time approx(s)	0.0608	0.0471	0.0496	0.0529	0.0354	0.0583	0.0721	0.0650	0.0800
error(percent)	1.2	0.13	0.83	0.11	0.83	0.41	0.25	0.31	0.45

Table 4-6: Retrieved interval times, exact interval times and percentage errors. Base subsurface model, data computation and recursive method parameters are used.

In Table 4-6, it can be seen that the retrieved intervaltimes t_1 till t_9 approximate the exact interval times well. The percentage errors lie between 0.11 and 1.2 percent.

With these intervaltimes the local reflection coefficients are retrieved. In Figure 4-7 the retrieved approximated local reflection coefficients are shown together with the exact local reflection coefficients. In Table 4-7, the approximated local reflection coefficients are shown together with the exact reflection coefficients, absolute errors and percentage errors.

In Table 4-7, it can be seen that the retrieved local reflection coefficients approximate the exact local reflection coefficients well. The relative errors lie between 0.15 and 5.2 percent with a mean relative error of 3.0 percent and a standard deviation of 1.95. The absolute errors lie between 0.0003 and 0.0039 with a mean absolute error of 0.0022 and a standard deviation of 0.0012. This means that the spread in absolute errors is less than the spread of percentage errors. This is due to the fact that the made absolute errors do not vary as much as the sizes of the reflection coefficients that have to be retrieved.

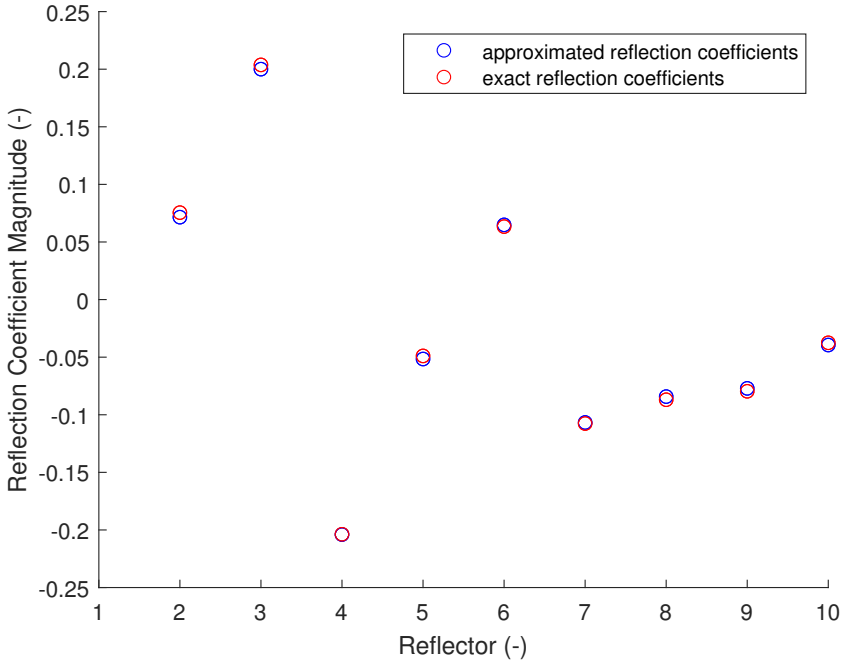

Figure 4-7: Approximated and exact local reflection coefficients. Base subsurface model, data computation and recursive method parameters are used. Reflectors 1 till 10 on the X-axis correspond to reflectors z_0 till z_9 respectively.

	z_1	z_2	z_3	z_4	z_5	z_6	z_7	z_8	z_9
r exact	0.0755	0.2037	-0.2037	-0.0489	0.0634	-0.1076	-0.0870	-0.0796	-0.0375
r approx	0.0715	0.2000	-0.2040	-0.0516	0.0649	-0.1067	-0.0842	-0.0771	-0.0395
abs error (-)	0.0039	0.0037	0.0003	0.0027	0.0015	0.0009	0.0027	0.0025	0.0019
error (percent)	5.2	1.8	0.15	5.5	2.4	0.86	3.1	3.1	5.1

Table 4-7: Approximated local reflection coefficients, exact local reflection coefficients and absolute errors and percentage errors. Base subsurface model, data computation and recursive method parameters are used.

4-4-2 Subsurface Model Parameter Variation

The recursive method is being compared with the exact solution while only varying subsurface model parameters. The parameter variation of the subsurface model is specified as shown in Table 4-8. Base data computation and base recursive method parameters are used.
As can be seen in Table 4-8, first the height of the layers is being varied by multiplying the heights of the base subsurface model with factors 1 till 5. Then the density of the layers will be varied by multiplying the densities of the base model with factor 0.75, 1 and 1.25.

Parameters Subsurface Model	Values
Heights of the model (m)	1 till 5 multiplied with the heights of the base model
Densities of the model (kg/m^3)	0.75,1,1.25 multiplied with the densities of the base model.

Table 4-8: Subsurface model parameter variation

In Figure 4-8, a plot of the RMS error of the 9 retrieved local reflection coefficients is shown for each factor that the heights of the base model have been multiplied with.

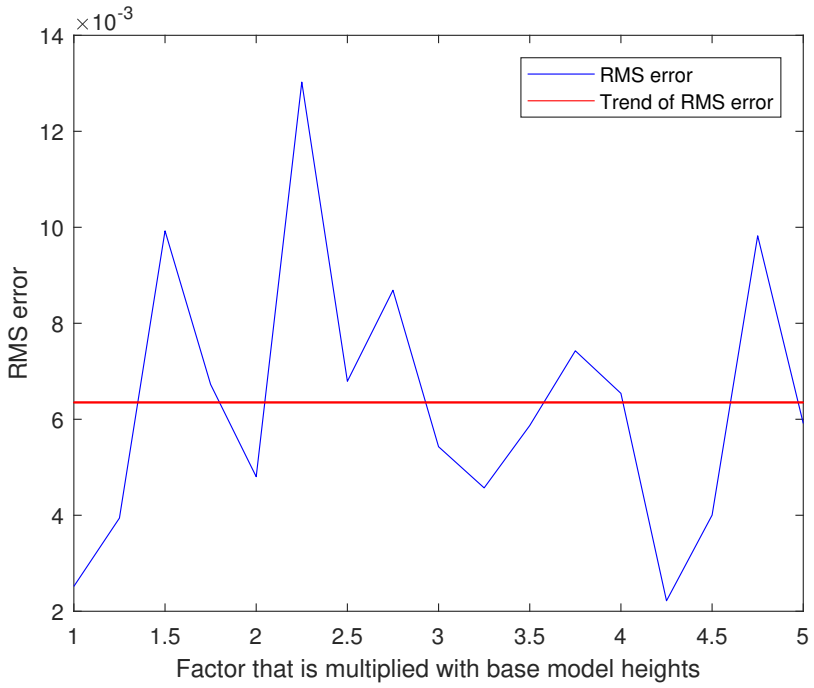

Figure 4-8: RMS error of the 9 retrieved local reflection coefficients for base subsurface model heights multiplied with factors 1 till 5. Base data computation and recursive method parameters are used.

In Figure 4-8, it can be seen that increasing the model heights results in a stable horizontal trend of RMS errors for the 9 retrieved local reflection coefficients. The RMS error value of this horizontal trend is 0.0064 with a standard deviation of 0.0028. This is to be expected since the recursive Marchenko inversion method is not sensitive to increasing times between arrivals in the reflection response.
When multiplying the base model heights with a factor lower than 1, resolution problems arise causing the method to not be able to retrieve any reflection coefficients. This is due to the fact that the decreased distance between reflectors causes sampling problems when the wavelength of the wavelet is too high to sample the shallow distance between reflectors correctly.

RMS errors of the 9 retrieved local reflection coefficients for each factor that the densities of the base model have been multiplied with, are given in Table 4-9.

Factor multiplied with densities of the base model	0.75	1	1.25
RMS error of the retrieved 9 reflection coefficients	0.0025	0.0025	0.0024

Table 4-9: RMS error of the 9 retrieved local reflection coefficients for base subsurface model densities multiplied with factors 0.75, 1 and 1,25. Base data computation and recursive method parameters are used.

In Table 4-9, it can be seen that changing the densities of the base model by multiplying them with factors 0.75, 1 and 1.25 results in stable RMS errors of the 9 retrieved local reflection coefficients.
The factors 0.75 till 1.25 have been chosen to keep realistic density values for the different layers of the model.

4-4-3 Data Computation Parameter Variation

The recursive method is being compared with the exact solution while only varying data computation parameters. The parameter variation of the data computation is specified as shown in Table 4-10. Base subsurface model and base recursive method parameters are used.

Parameters Measurement	Values
center wavelet frequency (Hz)	20,30,40,50,60,70,80,90,100

Table 4-10: Data computation parameter variation

The wavelet center frequency is being varied from 20Hz to 100Hz in steps of 10Hz as shown in Table 4-10

In Figure 4-9, the RMS error of the 9 retrieved local reflection coefficients is shown for each different wavelet center frequency used for data computation.
In Figure 4-9, it can be seen that the center wavelet frequency does influence the RMS errors for the 9 retrieved local reflection coefficients. After a center frequency wavelet of 40Hz and higher is used, the RMS error stabilizes. For lower frequencies, the RMS error quickly rises because of the too low frequency used to accurately sample the reflectors of the base subsurface model.

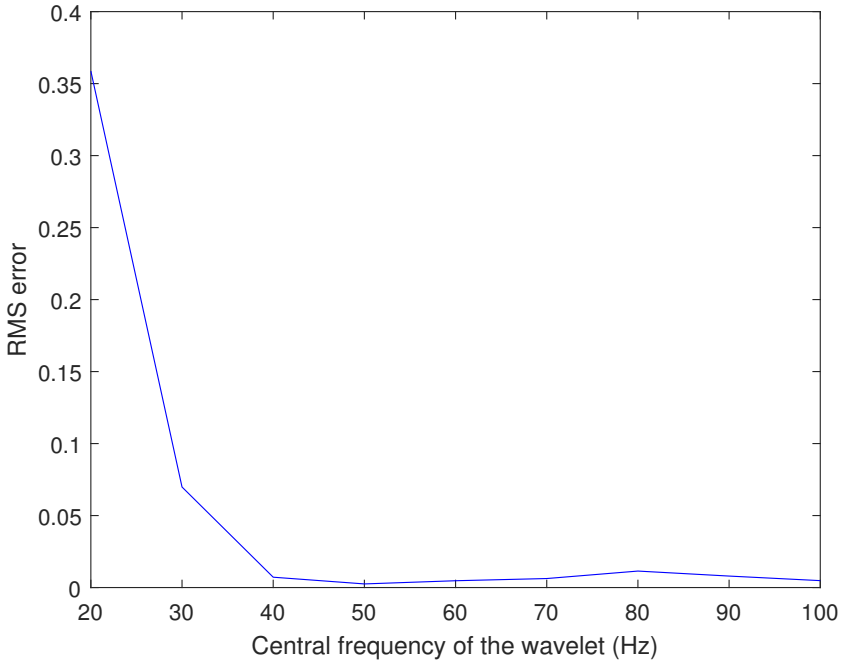

Figure 4-9: RMS error of the 9 retrieved local reflection coefficients for central wavelet frequencies of 20 till 100 Hz. Base subsurface model and recursive method parameters are used.

4-4-4 Recursive Method Parameter Variation

The influence of the recursive method parameters on the accuracy of the recursive Marchenko inversion method compared to the exact solution is investigated now. Base subsurface model and base data computation parameters are used. The parameter variation of the recursive method is specified as shown in Table 4-11.

Parameters method	Values
First focusing level of the method is located below reflector (-)	z_0 till z_8
Time subtracted or added to second interval time (s)	-10 till 10 times Δt

Table 4-11: Recursive method parameter variation

Instead of changing the the parameters (Table 4-4), that the recursive method uses to find first arrivals of the retrieved Green's function, a timing error is added to the second interval time t_2 without being compensated and then the RMS error of the found 9 reflection coefficients is computed. This is being done because the result of changing the parameters of the recursive method is that an error is added to an interval time. It is the influence of one interval time error on the RMS error of all the retrieved local reflection coefficients that is investigated.
In Figure 4-10, the RMS errors of the retrieved 9 local reflection coefficients are shown for different errors of the second interval time, t_2.

The errors are being induced by either adding or subtracting a number of Δt timing errors to interval time t_2.

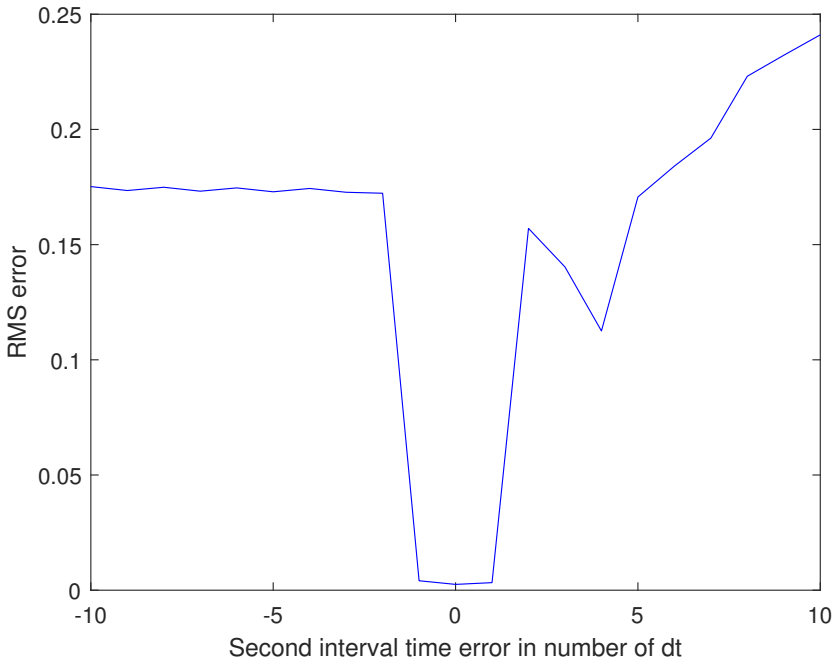

Figure 4-10: RMS error of the 9 retrieved local reflection coefficients for an over or an underestimation of the second interval time by 1 till 10 Δt. Base subsurface model and data computation parameters are used.

Error of the second interval time in Δt	-2	-1	0	1	2
RMS error of the retrieved 9 reflection coefficients	0.17	0.0041	0.0025	0.0033	0.16

Table 4-12: RMS error of the 9 retrieved local reflection coefficients for an over or underestimation of second interval time by 1 or 2 Δt. Base subsurface model and data computation parameters are used.

As can be seen in Figure 4-10 and Table 4-12, the RMS error of the 9 retrieved local reflection coefficients quickly rises after an overestimation of more than $1\Delta t$ is being used for the second interval time t_2. Also it can be seen that the RMS error of the 9 retrieved local reflection coefficients quickly rises after an underestimation of more than $1\Delta t$ is being used for the second interval time t_2. The lowest RMS error of the 9 retrieved local reflection coefficients is achieved when there is no under or overestimation of t_2 at all.

It can be concluded that since the recursive Marchenko inversion method uses a recursive scheme, it is prone to error buildup with increasing focusing depth. This could easily lead to a high error buildup if one interval time contaminated with an error is used.

In the next part, it is investigated how the number of recursion loops influences the accuracy of the retrieved reflection coefficients by the recursive method. This is being done by focusing at increasingly deeper reflectors by solving the coupled Marchenko equations before recursion takes place.
Changing the focusing level has as a result that less reflection coefficients can be retrieved with the recursive method. This means that an ever smaller number of reflection coefficients is retrieved. This means that the RMS error is being calculated of an increasingly smaller number of absolute errors.

In Table 4-13, the RMS errors of the retrieved local reflection coefficients are shown for a lowering of the first focusing level. Also the number of local reflection coefficients retrieved by the recursive Marchenko inversion method is shown.

First focusing level	z_0	z_1	z_2	z_3	z_4	z_5	z_6	z_7	z_8
Number of r	9	8	7	6	5	4	3	2	1
RMS error	0.0025	0.0022	0.0028	0.0037	0.0037	0.0031	0.0035	0.0037	0.0030

Table 4-13: RMS errors of the retrieved reflection coefficients depending on first focusing level. For clarification also the number of reflection coefficients that are used for RMS error calculation is shown. This number of reflection coefficients equals the number of recursion loops done by the method. Base subsurface model and data computation parameters are used.

In Table 4-13, it can be seen that less recursion iterations result in stable RMS errors of the retrieved local reflection coefficients. RMS errors stay lower than 0.0037. It can be concluded from Table 4-13 that the recursive Marchenko inversion method retrieves low error results independent of the number of recursion loops done. This is only true however, if the right first arrival times of the Green's function are found resulting in correct retrieved interval times.

4-5 Comparison between Recursive Method and Non-Recursive Method

In this section, the local reflection coefficients that are retrieved by using the non-recursive Marchenko inversion method are compared with the local reflection coefficients that are retrieved by using the recursive Marchenko inversion method. Also the computational cost of both methods will be compared. This will be done by running both inversion methods with the base subsurface model, base data computation and base recursive method parameters. Then the runtime of each method and the RMS errors of the 9 retrieved reflection coefficients will be compared.

First, the RMS error of the retrieved reflection coefficients of reflector z_1 till z_9 from the recursive Marchenko inversion method and the non-recursive Marchenko inversion method, are being compared. The RMS errors are shown in Table 4-14. In Table 4-14, it

	Recursive method	Non-recursive method
RMS error of the retrieved 9 reflection coefficients	0.0025	0.0057

Table 4-14: RMS error of the 9 retrieved local reflection coefficients for both recursive and non-recursive Marchenko inversion methods. Base subsurface model, data computation and method parameters are used.

can be seen that the RMS error of the 9 retrieved reflection coefficients from the recursive method are lower than the RMS error of the 9 retrieved reflection coefficients from the non-recursive method.

The computational cost of both recursive and non-recursive Marchenko inversion methods is also compared. This is done by running the 2 methods 3 times and comparing their run times. The runtimes are shown in Table 4-15.

Run	1	2	3
Runtime non-recursive method (s)	123.0196	118.1946	112.3449
Runtime recursive method (s)	2.3006	2.4075	2.3432

Table 4-15: Runtimes of both recursive and non-recursive Marchenko inversion methods. Base subsurface model, data computation and method parameters are used.

In Table 4-15 it can be seen that, as expected, the recursive Marchenko inversion method has a much lower computational cost than the non-recursive Marchenko inversion method.

Chapter 5

Conclusions

In this thesis, a recursive Marchenko inversion method has been successfully implemented and analysed. This Marchenko inversion method uses a recursive scheme to focus at ever deeper reflectors and retrieve reflection coefficients of these reflectors. It has been shown that the method delivers high accuracy results. It has also been shown that the recursive method has an advantage in computational expense compared with the existing, non-recursive Marchenko inversion method. Certain assumptions have been made though for this new recursive Marchenko inversion method. Among these are normal incidence of waves and piecewise constant impedances through the subsurface model.

Since the recursive Marchenko inversion method uses a recursive scheme, error buildup is a risk of this method. Error buildup will occur when a wrong interval time is found and used for the recursion to move the level of focus to a deeper reflector.

To mitigate this risk of error buildup, it is important to have an algorithm that can accurately pick first arrivals of the retrieved Green's functions. This is since the first arrival of the retrieved Green's functions is the controlling factor in generating correct interval times.

However, the recursive Marchenko inversion method has a big advantage. It has been proven that the recursive method can retrieve overestimations of interval timing errors and then compensate these accordingly. This can be done by looking at the reflection coefficient function. This is a new function found in this thesis. An overestimation of an interval time results in a time shift of the highest amplitude of this function away from zero time into negative times. This time shift has the exact magnitude of the overestimation of the interval time. It is this knowledge that is used to compensate for overestimations of the interval times. This in turn prevents errors to build up through the recursion. Because of the fact that only overestimation magnitudes can be found in the reflection coefficient function, the recursive Marchenko inversion method always uses an overestimation of the interval times and uses the reflection coefficient function to correct these interval times when necessary.

In the numerical results of this thesis, it has been shown that the absolute errors of the retrieved local reflection coefficients do not vary as much as the magnitude differences between the reflection coefficients that are being approximated. This results in a smaller spread in exact errors compared to the spread in percentage errors made by the recursive method.

It has also been shown that the accuracy of the found local reflection coefficients by the recursive Marchenko inversion method is stable under subsurface model variability and data computation variability as long as resolution is sufficient for the sampling of the subsurface model.

Finally and most importantly, the accuracy of the recursive Marchenko inversion method was tested under recursive method variability. In this section, the influence of not compensated interval timing errors on the RMS error of the found reflection coefficients has been analysed. It has been found that over and underestimations of the interval time used for recursion result in rapid error build up through the recursion.

For the future it may be interesting to implement the recursive Marchenko inversion method in a more realistic data computation environment in which a free surface of acquisition is modeled. Also the method can be implemented in 2D. A third possibility that can be explored is the implementation of the method on electromagnetic GPR data.

Bibliography

[Berkhout and Verschuur, 2005] Berkhout, A. and Verschuur, D. (2005). Removal of internal multiples with the commonfocus-point (cfp) approach: Part 1 explanation of the theory. *Geophysics*, 70(3):V45:V60.

[Broggini et al., 2012] Broggini, F., Snieder, R., and Wapenaar, K. (2012). Focusing the wavefield inside an unknown 1d medium: Beyond seismic interferometry. *Geophysics*, 77, no. 5:A25A28.

[Broggini et al., 2014] Broggini, F., Wapenaar, K., van der Neut, J., and Snieder, R. (2014). Data-driven greens function retrieval and application to imaging with multidimensional deconvolution. *Journal of Geophysical Research: Solid Earths*, 119:425:441.

[Cypriano et al., 2015] Cypriano, L., Marpeau, F., Brasil, R., Welter, G., Prigent, H., Douma, H., Velasques, M., Boechat, J., de Carvalho, P., Guerra, C., Theoro, C., Martini, A., and Cruz, J. N. (2015). The impact of inter-bed multiple attenuation on the imaging of pre-salt targets in the santos basin off-shore brazil. *77th Annual International Conference and Exhibition, EAGE, Extended Abstracts*, N114.

[Fleury, 2012] Fleury, C. (2012). Wave propagation in complex media, scattering theory, and application to seismic imaging. *Colorado School of Mines*.

[Goupillaud, 1961] Goupillaud, P. L. (1961). An approach to inverse filtering of near-surface layer effects from seismic records. *Geophysics*, 26(6):754.

[Griffiths et al., 2011] Griffiths, M., Hembd, J., and Prigent, H. (2011). Applications of interbed multiple attenuation. *The Leading Edge*, 30:906:912.

[Hubral et al., 1980] Hubral, P., Treitel, S., and Gutowski, P. R. (1980). A sum autoregressive formula for the reflection response. *Geophysics*, 45, No. 11:1697:1705.

[King et al., 2013] King, S., Dyer, R., and O'Neill, P. (2013). Data-driven internal multiple attenuation: Theory and examples. *83rd Annual International Meeting, SEG*, 4096:4093.

[Matson et al., 1999] Matson, K., Corrigan, D., Weglein, A., Young, C., and Carvalho, P. (1999). Inverse scattering internal multiple attenuation: Results from complex synthetic and field data examples. *89th Annual International Meeting, SEG*, Expanded Abstracts:1060:1063.

[Oristaglio, 1989] Oristaglio, M. L. (1989). An inverse scattering formula that uses all the data. inverse problems. *Inverse Problems*, 5(6):1097.

[Robinson and Treitel, 1978] Robinson, E. A. and Treitel, S. (1978). The fine structure of the normal incidence synthetic seismogram. *Geophysical Journal of the Royal Astronomical Society*, 35:289:309.

[Rose, 2002] Rose, J. (2002). Single-sided autofocusing of sound in layered materials. *Inverse Problems*, 18:1923:1934.

[Singh et al., 2015] Singh, S., Snieder, R., Behura, J., van der Neut, J., Wapenaar, K., and Slob, E. (2015). Marchenko imaging: Imaging with primaries, internal multiples, and free-surface multiples. *GEOPHYSICS*, 80, NO. 5:S165:S174.

[Singh et al., 2017] Singh, S., Snieder, R., van der Neut, J., Thorbecke, J., Slob, E., and Wapenaar, K. (2017). Accounting for free-surface multiples in marchenko imaging. *GEOPHYSICS*, 82:R19–R30.

[Slob and Wapenaar, 2014] Slob, E. and Wapenaar, K. (2014). Data-driven inversion of gpr surface reflection data for lossless layered media. *The 8th European Conference on Antennas and Propagation (EuCAP 2014)*, pages 3378–3382.

[Slob et al., 2014] Slob, E., Wapenaar, K., Broggini, F., and Snieder, R. (2014). Seismic reflector imaging using internal multiples with marchenko-type equations. *GEOPHYSICS*, 79(2):S63–S76.

[Song et al., 2013] Song, J., Verschuur, E., and Chen., X. (2013). Comparing three feedback internal multiple elimination methods. *Journal of Applied Geophysics*, 95:66–76.

[Stakgold and Holst, 2011] Stakgold, I. and Holst, M. J. (2011). Green's functions and boundary value problems. *John Wiley and Sons*.

[Wapenaar et al., 2014] Wapenaar, K., Thorbecke, J., van der Neut, J., Broggini, F., Slob, E., and Snieder, R. (2014). Marchenko imaging. *GEOPHYSICS*, 79(3).

[Weglein et al., 1997] Weglein, A. B., Gasparotto, F. A., Carvalho, P. M., and Stolt, R. H. (1997). An inverse scattering series method for attenuating multiples in seismic reflection data. *Geophysics*, 62:1975:1989.